

## Water-network percolation transitions in hydrated yeast

Dagmara Sokołowska, Agnieszka Król-Otwinowska, and Józef K. Mościcki

*Smoluchowski Institute of Physics, Jagiellonian University, Reymonta 4, 30-059, Krakow, Poland*

(Received 12 March 2004; revised manuscript received 11 June 2004; published 3 November 2004)

We discovered two percolation processes in succession in dc conductivity of bulk baker's yeast in the course of dehydration. Critical exponents characteristic for the three-dimensional network for heavily hydrated system, and two dimensions in the light hydration limit, evidenced a dramatic change of the water network dimensionality in the dehydration process.

DOI: 10.1103/PhysRevE.70.052901

PACS number(s): 87.14.-g, 64.60.Ak, 72.80.-r

Several biological systems of increasing complexity, protein powders, biological membranes, seed endosperm, early crustacean embryos, and recently lichens, are known to demonstrate conductivity percolation at low hydration levels [1–4]. These systems resemble more or less structures of highly porous materials, e.g., of controlled pore glass, therefore a system which is difficult to model. In this study we turned our attention to hydrated yeast. Yeast is one of very few “standard” model systems used for various basic and applied fields of life science, medicine, bio-, and nanotechnology. Some of their mutants can be cultivated to grow in a restrictive shape [5], therefore providing information of the morphological dependence of physical properties under investigation. Last but not least, yeasts can be studied *in vivo*.

Although dielectric properties of aqueous suspensions of yeast have been intensively studied in the past [5–7], we are not aware of previous dc-conductivity studies of less hydrated yeast samples. Our study of baker's yeast (*Saccharomyces cerevisiae*) fills the gap. We observed two pronounced percolation phenomena in dielectric behavior and dc-conductivity as a function of hydration, one in heavily hydrated, and the other in lightly hydrated yeast. Here we report and discuss the values of critical exponents for both processes.

Industrial baker's yeast in bulk (different strains of *Saccharomyces cerevisiae* in moist form) was provided by Wytornia Drozdzy Piekarskich, Krakow, Poland. To preserve the moist yeast sample as well-defined model system in the course of the study, it was investigated in the hydration range securing viability of the cells. At one extreme ( $\sim 60\%$  w/w) the sample had—as verified by the polarized light microscope—a form of yeast globular cells tightly packed into an amorphous matrix. The free space between the cells formed a continuous network, filled up at this hydration with water (intercellular). At low extreme ( $\sim 10\%$  w/w), although we did not control the viability of yeast cells, hydration was well above 5% moisture, the commonly accepted dehydration limit for high viability of the cells [8]. Additionally, in order to secure viability of the cells in the course of study, dehydration was always very slow, executed via still air, thus eliminating the possibility of “osmotic shock” [9]. To sustain high viability of the cells, temperature of the system was kept in the range of 23–25°C [10]. We have no doubts that yeast cells always preserved their structural integrity and physical properties in the course

of this work, so we dealt with well-defined model system.

A parallel plate dielectric cell was made of two mirror-polished copper disks,  $d=47.9$  mm in diameter. To allow uniform dehydration of a sample, 56 circular holes, of radius  $r=1$  mm were made randomly in the upper electrode. The distance of  $l=3.5$  mm between the electrodes was fixed by Teflon spacers. The empty capacitor was calibrated with solutions of ethanol and saccharine; the empty cell capacitance was  $C_0=(8.57\pm 0.12)$  pF. Dielectric measurements were carried out on a Hewlett Packard 4192A impedance analyzer during sample dehydration. A laboratory balance WPS72 Radwag (Radom, Poland, systematic uncertainty  $\pm 2 \times 10^{-4}$  g) was used to continuously monitor the water content in the sample. The sample holder with the sample together with a hydrophilic substance (calcium chloride) was enclosed tightly in the balance chamber. A dehydration process was then carried out through the air in seclusion at the rate slightly varying in time. Dielectric spectra (10 Hz–10 MHz) were continuously taken every 5 min in the course of dehydration. Measurements repeated for six samples of different strains of yeast consistently gave, within experimental noise, the same results.

All dielectric spectra,  $\varepsilon^*(\omega)=\varepsilon'(\omega)-i\varepsilon''(\omega)$ , recorded for different water content in yeast showed on decreasing frequency well-separated contributions from three effects: a Maxwell-Wagner relaxation process, dc conductivity, and electrode polarization [6,11]. This allowed for accurate extraction of dc conductivity for all hydration levels studied.

dc conductivity  $\sigma$  and low-frequency dielectric constant  $\varepsilon_{LF}$  as functions of water mass fraction  $\rho_W=m_W/m$  (where  $m_W$  and  $m$  are water mass and the mass of the sample, respectively) are shown in Fig. 1. Three distinct hydration regions with different dc conductivity and  $\varepsilon_{LF}$  behavior can be isolated. In the course of initial dehydration of the heavily hydrated sample ( $\rho_W=0.5-0.7$ ) a drop in  $\sigma$  (two orders of magnitude) and  $\varepsilon_{LF}$  (one order) is dramatic. On further dehydration ( $\rho_W=0.2-0.5$ ) this decrease slows down but does not level out tending more or less to show a monotonous decrease of  $\sigma$  and  $\varepsilon_{LF}$  with dehydration. However, for lightly hydrated samples ( $\rho_W=0.1-0.2$ ),  $\sigma$  and  $\varepsilon_{LF}$  begin again to decrease rapidly over a narrow range of hydration (three orders of magnitude for  $\sigma$  and one order of magnitude for  $\varepsilon_{LF}$ ), cf. inset in Fig. 1. Of our particular interest are these two rapid decrease regions, referred to thereafter as region I and region II, respectively, where dc conductivity shows behav-

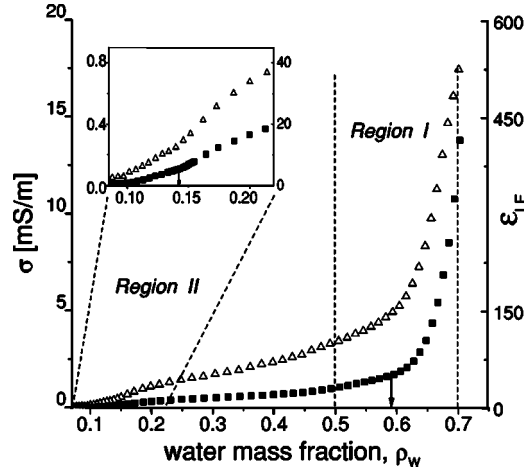


FIG. 1. dc conductivity  $\sigma$  (■, left axis) and low-frequency permittivity  $\epsilon_{LF}$  ( $\Delta$ , right axis) vs water mass fraction  $\rho_W$  in the hydrated yeast.

ior characteristic for conductivity percolation phenomena.

For a classic, site-percolation two-phase network case, the dc conductivity of the network has a power-law dependence on the departure from the threshold concentration  $p$  of the conducting species. In the vicinity of the percolation threshold,  $p^*$  [12]:

$$\begin{aligned} \sigma(p) &\propto (p - p^*)^t, & p \geq p^*, \\ \sigma(p) &\propto (p^* - p)^{-s}, & p \leq p^*, \end{aligned} \quad (1)$$

where values of critical exponents  $t$  and  $s$  reflect dimensionality of the network. Application of Eqs. (1) to real experimental data usually requires identification of relationships between measurable quantities and the model  $\sigma$  and  $p$ .

The hydrated yeast under investigation is a bulk, heterogeneous system. Just above the upper limit of region I, the system can be regarded as an amorphous tightly packed matrix of more or less monodisperse in shape globular objects. The free space between the objects forms a quite spacious network filled completely by a conducting medium—intercellular water. As the sample begins to lose water, the continuous system initially breaks down into regions of tight-packed yeast cells and completely empty “voids.” Probably at the same time organization of yeast cells in the tight-packed regions tends to the close-packing limit, and the material reaches stable, more or less porous bicontinuous structure of intermingling the yeast cells and water networks. This is roughly where region I begins.

The fall of  $\sigma$  is generally more pronounced, and starts just before the offset of  $\epsilon_{LF}$  decreases, somewhat similarly to percolation observed in microemulsions [13]. This is indicative of the intercellular water matrix being the one on which percolation takes place in the course of dehydration. Notably, the conductivity does not fall to zero below the percolation threshold: although the infinite cluster of the intercellular water network disappeared, the remaining water wetting the scaffolding of yeast material sustains some “remnant” conductivity.

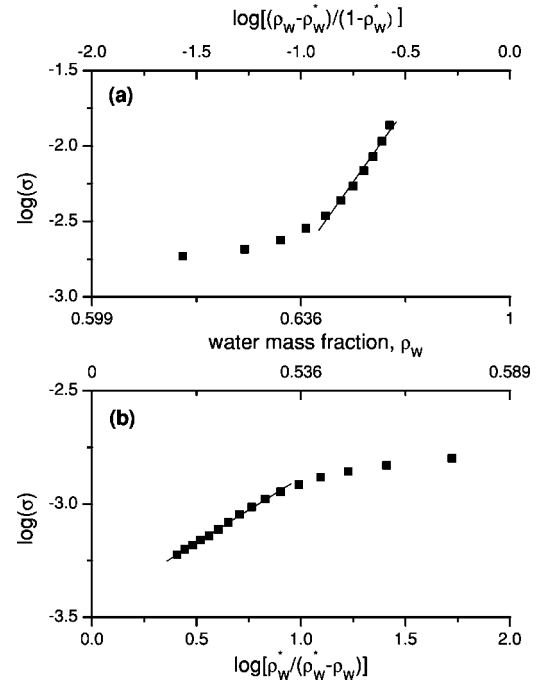


FIG. 2. Conductivity percolation in the heavily hydrated yeast (Region I). (a)  $\log_{10}(\sigma)$  vs  $\log_{10}[(\rho_W - \rho_W^*) / (1 - \rho_W^*)]$  (top axis) above the percolation threshold,  $\rho_W > \rho_W^*$ . The straight line is Eq. (2a) fit with  $t = 1.94 \pm 0.11$ . (b)  $\log_{10}(\sigma)$  vs  $\log_{10}[\rho_W^* / (\rho_W - \rho_W^*)]$  (bottom axis) below the percolation threshold,  $\rho_W < \rho_W^*$ . The straight line is Eq. (2b) fit with  $s = 0.57 \pm 0.01$ .

The volume fraction of intercellular water “conductors”  $\phi$  is therefore directly proportional to the site occupancy probability  $p$  of our interest. The relationship between conductivities of intercellular water  $\sigma_W$ , of the remnant conductivity  $\sigma_Y$ , and of the mixture of the two components  $\sigma$ , in the vicinity of percolation threshold should then follow [14,15]

$$|\sigma_W| \rightarrow \infty: \sigma = \sigma_Y \frac{(\phi^*)^s}{(\phi^* - \phi)^s}, \quad \phi < \phi^* - \delta_1, \quad (2a)$$

$$|\sigma_Y| \rightarrow 0: \sigma = \sigma_W \frac{(\phi - \phi^*)^t}{(1 - \phi^*)^t}, \quad \phi > \phi^* + \delta_2, \quad (2b)$$

where  $\phi^*$  is the volume fraction intercellular water at the percolation threshold. In addition to Eqs. (2), the “width” of

TABLE I. Comparison between critical exponents from this work and experimental and model literature data for 3D network percolation.

Critical expt.	This work Region I	3D percolation		
$t$	$1.94 \pm 0.11$	$2.24^a$	$1.9 \pm 0.1^b$	$1.94^c$ $2.00^d$
$s$	$0.57 \pm 0.01$	$0.44^a$	$0.75 \pm 0.04^b$	$1.2^c$ $0.73^d$

<sup>a</sup>J. M. Luck [19].

<sup>b</sup>References in Ref. [19].

<sup>c</sup>Dynamic percolation; G. S. Grest *et al.* [20].

<sup>d</sup>D. Stauffer and A. Aharony [12].

TABLE II. Critical exponents for two-dimensional conductivity percolation of resistor lattices.

Critical exp.	This work Region II		2D percolation					
$t$	$1.08 \pm 0.02$	$1.10 \pm 0.05^a$	$1.25 \pm 0.05^b$	$1.3^c$	$1.135^d$	$1.18^e$	$1.23^f$	$1.29^g$
$s$	$0.98 \pm 0.01$	$1.1^a$	$1.10 \pm 0.15^b$	$1.3^c$	$1.135^d$			

<sup>a</sup>Bond [22].<sup>b</sup>Site [22].<sup>c</sup>D. Stauffer and A. Aharony [12].<sup>d</sup>J. M. Luck [19].<sup>e</sup>In lichens [1].<sup>f</sup>In maize seeds [2].<sup>g</sup>In protein lysozyme powders [18].

the transition range around the percolation threshold is expected to be of order of [14]

$$\Delta = \delta_1 + \delta_2 = \left( \frac{\sigma_Y}{\sigma_W} \right)^{1/(t+s)} \quad (3)$$

and conductivity of the mixture at the percolation threshold [15]

$$\sigma^* = \sigma_W \left( \frac{1 - \phi^*}{\phi^*} \right)^{-st/s+t} \left( \frac{\sigma_Y}{\sigma_W} \right)^{t/s+t}. \quad (4)$$

At the low hydration level (region II) the material made up of close-packed yet viable yeast cells has high porosity. The situation does not depart significantly from that observed, e.g., in silicates [16]. The conductivity behavior shows significant similarities to results from other biological [1–4] and similar model materials [16,17]. Since the water content in the material is still well above the osmotic shock level, there must be enough water in the system to at least moisten the cells outer surfaces (the skin of remnant intercellular water). We assume therefore that hydration level  $h = m_W/m_0$  (where  $m_W$  and  $m_0$  are the skin water mass and the sample dry mass, respectively) are directly proportional to the site occupancy probability of the water network  $p$ , and Eqs. (1) become [18]

$$\frac{\sigma - \sigma^*}{\sigma^*} \propto (h - h^*)^t, \quad h > h^*, \quad (5a)$$

$$\frac{\sigma^* - \sigma}{\sigma^*} \propto (h^* - h)^s, \quad h < h^*, \quad (5b)$$

where  $\sigma^*$  is a nonpercolating, background component of total conductivity at the threshold. Again, Eqs. (5) are valid only in vicinity of the percolation threshold [18].

Results of fitting experimental data in region I with Eqs. (2a) and (2b) are shown in Figs. 2(a) and 2(b), respectively. (Note that the volume fraction  $\phi$  is replaced by water mass fraction  $\rho_W$  in Figs. 2(a) and 2(b); due to very similar densities of water and moist yeast such substitution can be done without a substantial penalty.) The best fit (Levenberg-Marquardt) yields the percolation threshold at  $\rho_W^* = 0.595$ , critical exponents  $t = 1.94 \pm 0.11$  and  $s = 0.57 \pm 0.01$ , and material conductivities  $\sigma_W = 0.17 \pm 0.03$  S/m and  $\sigma_Y = (3.49 \pm 0.06) \times 10^{-4}$  S/m. Self-consistency of these results was additionally cross checked with the aid of Eqs. (3) and

(4), and close inspection of Figs. 1 and 2. Equation (3) yields the transition interval  $\Delta = 0.09 \pm 0.01$  which compares well with 0.13 estimated from Figs. 2(a) and 2(b). Analogously compares  $\sigma^*$ , obtained from Eq. (4), and estimated from Fig. 1:  $1.7 \pm 0.6$  and  $2.32$  mS/m, respectively.

Critical exponents from region I compare well with a number of model predictions for the three-dimensional (3D) network, e.g., of Stauffer and Aharony [12], from the renormalization-group approach of Luck and several different alternative approaches, the results of which are summarized in Luck [19], as well as with critical exponents obtained from a model for dynamic percolation in microemulsions [20], cf. Table I. Our values of  $t$  and  $s$  coincide very nicely with the model values. Discrepancy in  $s$  between our and dynamic percolation exponents should be expected [20].

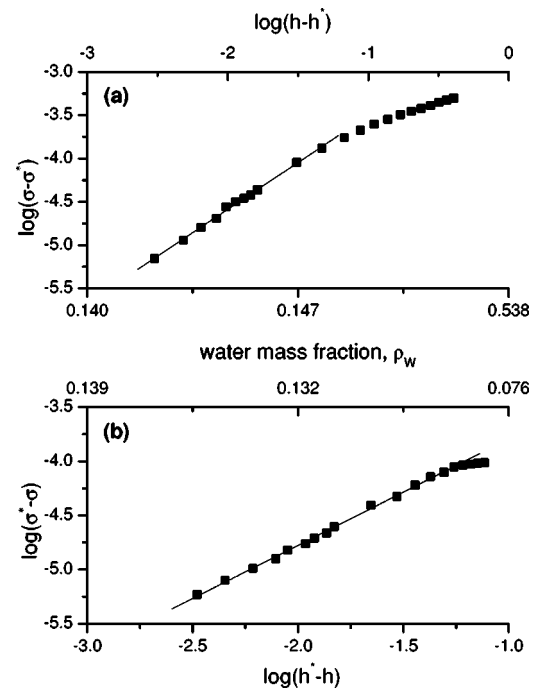


FIG. 3. Conductivity percolation in the lightly hydrated yeast (region II). (a)  $\log_{10}(\sigma - \sigma^*)$  vs  $\log_{10}(h - h^*)$  (top axis) above the percolation threshold,  $h > h^*$ . The straight line is Eq. (5a) fit with  $t = 1.08 \pm 0.02$ . (b)  $\log_{10}(\sigma^* - \sigma)$  vs  $\log_{10}(h^* - h)$  (bottom axis) below the percolation threshold,  $h < h^*$ . The straight line is Eq. (5b) fit with  $s = 0.98 \pm 0.01$ .

In region II,  $\rho_w=0.1-0.2$ , dc conductivity of yeast was successfully fitted with Eqs. (5a) and (5b), respectively. The best-fit (Levenberg-Marquardt) values of the percolation threshold and critical exponents are  $h^*=0.302$  (equivalent of  $\rho_w^*=0.14$ ),  $t=1.08\pm 0.02$ , and  $s=0.98\pm 0.01$ , respectively (cf. Fig. 3). Comparison of these critical exponents with available literature data indicates that we evidenced percolation on 2D conducting network, cf. Table II. First of all, the values of  $s$  and  $t$  for yeast are in accord with predictions for many model 2D networks, obtained by various methods. The value of the critical exponent  $t$  is also very close to the one observed for biological materials (lichens, powders of protein lysozyme, embryos, and endosperms of maize) with presumably 2D protonic conductivity [1,2,18]. In yeast, in addition to the protonic contribution on the outer yeast cell surface, there must also be an ionic contribution to the conduction process, executed via, e.g., the cells interior and then through contact points between cells.

How can one rationalize our observations? The conducting bulk of the heavily hydrated yeast sample is bicontinuous: one component is made of tightly packed, low conducting, and relatively large yeast cells ( $5\ \mu\text{m}\times 6\ \mu\text{m}$ ) and the second component is the filament of the free space remaining between the cells. The filament is a solution of minerals and ions in water [21]. The conducting interior of a cell (cytoplasm) is isolated from the solution by an almost noncon-

ducting plasma membrane and a thick, carbon rich cell wall with limited permeability. The charge transport through the material is complex and realized via three conduction pathways: via intercellular water network, on the cell surface, and through the intracellular material, in addition to a number of different charge carriers involved on each of the pathways, the intercellular water network being clearly the dominating one. On dehydration intercellular water evacuates first, more and more voids are created in the free space between yeast cells, and at some point this intercellular water network gets destroyed in the region I percolation process. Or, more precisely, it is replaced by a new, continuous, infinite skin water network formed on the outer surface of the close-packed yeast cells. A completely different geometry of charge transport pathways becomes eminent. Continuing the dehydration process towards the light hydration limit, at some point, there is no more intercellular mobile water left in the system, and the cells outer surface begins finally to dry out, and even this continuous network of skin water breaks down (region II) as the system goes across the light hydration percolation threshold.

We have benefited from the valuable discussions of H. Haranczyk. Financial support from the Polish State Committee for Scientific Research (KBN) under Project No. 2 P03B 086 23 is acknowledged.

- 
- [1] H. Haranczyk, M. Wnek, M. Olech, and J. K. Moscicki (unpublished).
  - [2] F. Bruni, G. Careri, and A. C. Leopold, *Phys. Rev. A* **40**, 2803 (1989).
  - [3] J. A. Rupley, L. Siemiankowski, G. Careri, and F. Bruni, *Proc. Natl. Acad. Sci. U.S.A.* **85**, 9022 (1988).
  - [4] M. Settles, W. Doster, F. Kremer, F. Post, and W. Schirmacher, *Philos. Mag. B* **65**, 861 (1992).
  - [5] K. Asami, *Biochim. Biophys. Acta* **1472**, 137 (1999).
  - [6] K. Asami, E. Gheorghiu, and T. Yonezawa, *Biochim. Biophys. Acta* **1381**, 234 (1998).
  - [7] X-B. Wang, Y. Huang, R. Holzel, J. P. H. Burt, and R. Pething, *J. Phys. D* **26**, 312 (1993).
  - [8] P. V. Attfield, S. Kletsas, D. A. Veal, R. van Rooijen, and P. J. Bell, *J. Appl. Microbiol.* **89**, 207 (2000).
  - [9] L. Beney, I. M. de Maranon, P.-A. Marechal, and P. Gervais, *Int. J. Food Microbiol.* **55**, 275 (2000).
  - [10] P. Gervais, P.-A. Marechal, and P. Molin, *Biotechnol. Bioeng.* **40**, 1435 (1992).
  - [11] T. Chelidze, *J. Non-Cryst. Solids* **305**, 285 (2002).
  - [12] D. Stauffer and A. Aharony, *Introduction to Percolation Theory*, 2nd ed. (Taylor and Francis, London, 1994).
  - [13] M. A. van Dijk, *Phys. Rev. Lett.* **55**, 1003 (1985).
  - [14] Z. Saidi, C. Mathew, J. Peyrelase, and C. Boned, *Phys. Rev. A* **42**, 872 (1990).
  - [15] D. S. McLachlan, W. D. Heiss, C. Chiteme, and J. Wu, *Phys. Rev. B* **58**, 13 558 (1998).
  - [16] D. Sokolowska, A. Krol-Otwinowska, and J. K. Moscicki (unpublished).
  - [17] S. J. Chen, D. F. Evans, B. W. Ninham, D. J. Mitchell, F. D. Blum, and S. Pickup, *J. Phys. Chem.* **90**, 842 (1986).
  - [18] G. Careri, A. Giansanti, and J. A. Rupley, *Phys. Rev. A* **37**, 2703 (1988).
  - [19] J. M. Luck, *J. Phys. A* **18**, 2061 (1985).
  - [20] G. S. Grest, I. Webman, S. A. Safran, and A. L. R. Bug, *Phys. Rev. A* **33**, 2842 (1986); M. W. Kim and J. S. Huang, *ibid.* **34**, 719 (1986); M. Moha-Ouchane, J. Peyrelase, and C. Boned, *ibid.* **35**, 3027 (1987).
  - [21] D. Batani *et al.*, *Eur. Phys. J. D* **21**, 167 (2002).
  - [22] J. P. Straley, *Phys. Rev. B* **15**, 5733 (1977).